

# CHEMISTRY

## A European Journal



### Accepted Article

**Title:** Bimodal heterogeneous functionality in redox-active conjugated microporous polymer towards electrocatalytic oxygen reduction and photocatalytic hydrogen evolution

**Authors:** Ashish Singh, Parul Verma, Debabrata Samanta, Tarandeep Singh, and Tapas Kumar Maji

This manuscript has been accepted after peer review and appears as an Accepted Article online prior to editing, proofing, and formal publication of the final Version of Record (VoR). This work is currently citable by using the Digital Object Identifier (DOI) given below. The VoR will be published online in Early View as soon as possible and may be different to this Accepted Article as a result of editing. Readers should obtain the VoR from the journal website shown below when it is published to ensure accuracy of information. The authors are responsible for the content of this Accepted Article.

**To be cited as:** *Chem. Eur. J.* 10.1002/chem.201904938

**Link to VoR:** <http://dx.doi.org/10.1002/chem.201904938>

Supported by  
**ACES**

WILEY-VCH

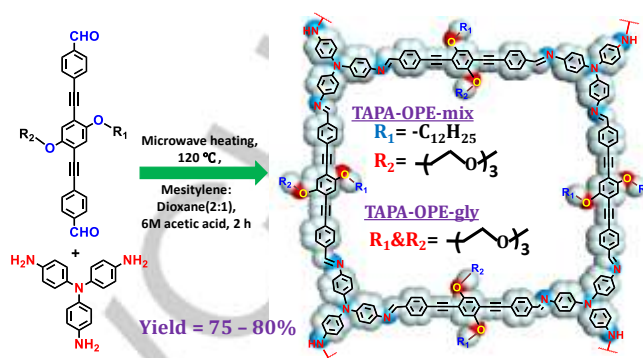
# Bimodal heterogeneous functionality in redox-active conjugated microporous polymer towards electrocatalytic oxygen reduction and photocatalytic hydrogen evolution

Ashish Singh, Parul Verma, Debabrata Samanta, Tarandeep Singh and Tapas Kumar Maji\*

**Abstract:** Designing and developing heterogeneous catalysts for conversion of renewable energy to chemical energies by electrochemical as well as photochemical processes are in the forefront of the energy research. Here, we have synthesized donor-acceptor based two new redox active conjugated microporous polymers (CMPs) namely; TAPA-OPE-mix and TAPA-OPE-gly via Schiff base condensation reaction using microwave synthesizer. Notably, asymmetric and symmetric bola-amphiphilic nature of OPE struts have resulted in distinct nano-structuring and morphologies in CMPs. Interestingly, both CMPs have shown impressive heterogeneous catalytic activity towards electrochemical O<sub>2</sub> reduction and photocatalytic H<sub>2</sub> evolution reactions and therefore, for the first time, turns out as bimodal electro and photo-catalyst porous organic material. Furthermore, redox-active property of CMPs was exploited for *in-situ* generation and stabilization of platinum nanoparticles (Pt) and subsequently, metal nano-particles stabilized CMPs (Pt@CMPs) exhibited significantly enhanced photocatalytic activity.

## Introduction

Globally increased energy demand and in contrary, rapid depletion in non-renewable energy sources stem a quest for alternate energy sources. In this direction, electrochemical and photo-chemical conversion of naturally abundant renewable resources (water and sun light) into chemical energy are considered to have potential to change the global energy landscape.<sup>[1-5]</sup> In electrocatalysis, electrochemical redox reactions operated at a certain potential on the electrode surface. This process has high significance in the energy conversion and storage systems such as fuel cells and in metal-air battery applications.<sup>[6-8]</sup> On the other hand, photocatalysis process dealt with the conversion of naturally abundant sun's light energy into chemical energy in the form of molecular hydrogen (H<sub>2</sub>).<sup>[9-13]</sup> Photochemical water splitting is considered to be one of the most promising sources for clean and sustainable energy to solve the energy crisis.<sup>[14, 15]</sup> Importantly, photochemical transformation of sun light to chemical energy are being naturally operated in green plants for millions of years and known as photosynthesis. However, sluggish reaction kinetics and subsequent use of precious metal-based catalysts for catalysing



Scheme 1: Synthetic scheme for CMPs; TAPA-OPE-mix and TAPA-OPE-gly.

electrochemical and photochemical reactions are found to be major limitations to employ these processes in a large scale.<sup>[16-19]</sup> Several materials such as metal oxides, phosphides, sulphides, chalcogenides, inorganic or organic-inorganic hybrid porous and carbon based materials are known in literature separately as either electrocatalyst<sup>[4, 20-28]</sup> or photocatalyst<sup>[14, 29-32]</sup> but purely organic based catalysts working as electro or photo-catalyst are rarely explored.<sup>[33-38]</sup>

Conjugated microporous polymers (CMPs) are found to be an emerging class of porous organic materials that have demonstrated treasure trove of applications.<sup>[39, 40]</sup> Owing to synthetic diversity and permanent micro-porosity, CMP materials have gained widespread attention in the realm of energy materials<sup>[41, 42]</sup>, heterogeneous catalysis and luminescent materials.<sup>[35, 43-47]</sup> Recently, designing redox-active CMP materials by integrating electron donor and acceptor organic struts has drawn immense interest as they have shown potential for catalysing electrochemical oxygen reduction (ORR) reaction<sup>[22, 41]</sup> which is a half-cell reaction in fuel cells and metal-air batteries.<sup>[6, 28]</sup> Moreover, redox active CMPs were also found to be capable for *in-situ* generation and stabilization of metal nano-particles (NPs) and subsequently, metal nano-particle stabilized CMP (NP@CMP) materials have shown significantly improved electro-catalytic activities.<sup>[22, 41]</sup> Furthermore, organic porous materials are recently being explored as heterogeneous catalysts for photochemical H<sub>2</sub> evolution reaction.<sup>[48-54]</sup> However, improvement in both these processes in a cost effective manner are forefront challenge for the scientific community.<sup>[55]</sup> To the best of our knowledge, CMP materials with bimodal functionality that can catalyses both, electrochemical ORR as well as photo-chemical H<sub>2</sub> evolution is yet to be documented. Therefore, exploration of bimodal functionality for catalysing both, electro- and photo-chemical reactions would broaden the applications of CMPs in view of designing metal free robust materials for addressing energy challenges. Another crucial parameter which plays pivotal role in catalytic performances and needs to be taken in to account is

Dr. A. Singh, P. Verma, Dr. D. Samanta, T. Singh, Prof. Dr. T. K. Maji  
Molecular Materials Laboratory, Chemistry and Physics of Materials Unit,  
School of Advanced Materials (SAMat),  
Jawaharlal Nehru Centre for Advanced Scientific Research, Bangalore-  
560064, India.  
E-mail: [tmaji@incasr.ac.in](mailto:tmaji@incasr.ac.in)  
Homepage: [www.incasr.ac.in/tmaji/](http://www.incasr.ac.in/tmaji/)  
Supporting information (SI) for this article is given via a link at the end of  
the document.

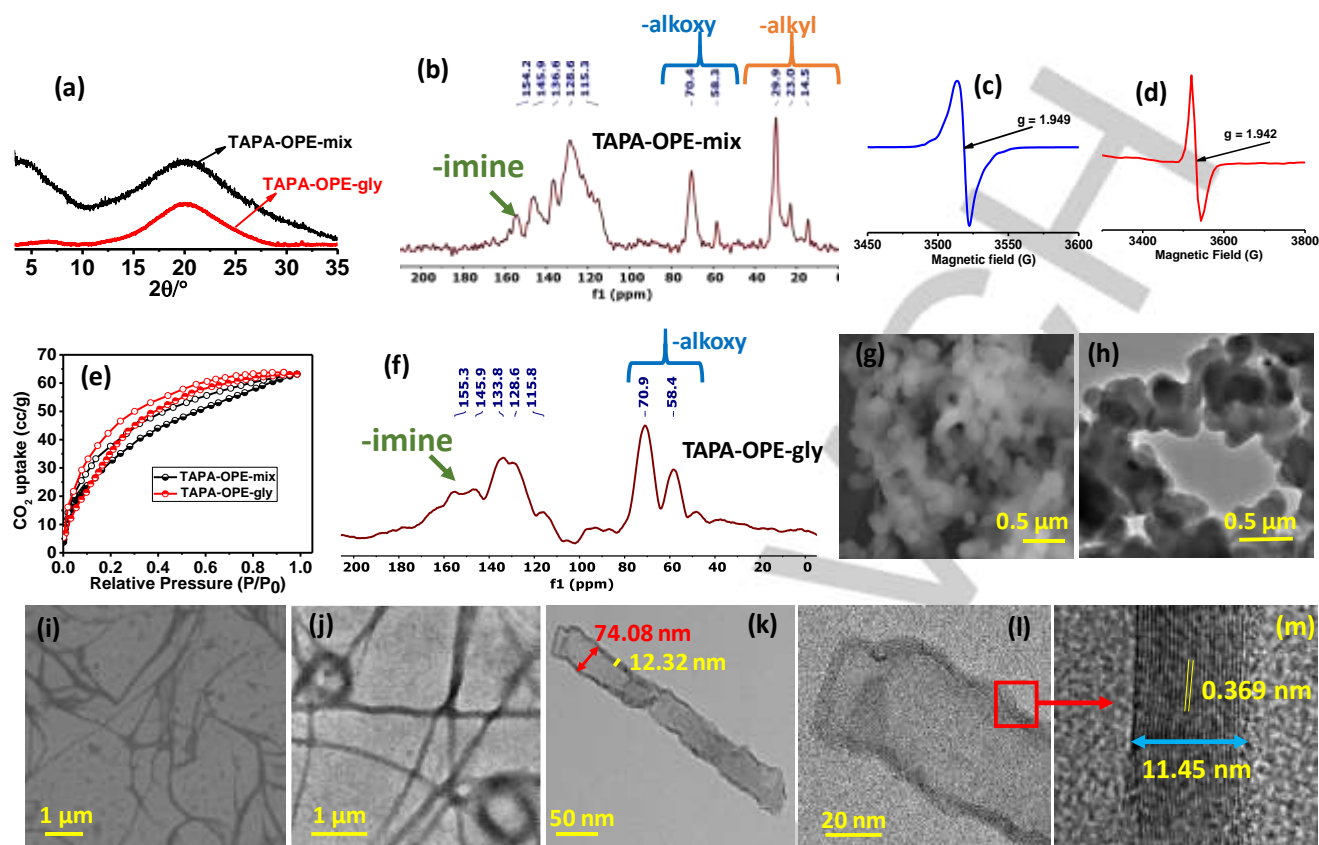


Figure 1: Characterizations of TAPA-OPE-mix and TAPA-OPE-gly: (a) PXRD for both CMPs; (b) solid-state  $^{13}\text{C}$  NMR for TAPA-OPE-mix; EPR spectrum (c) for TAPA-OPE-mix and (d) for TAPA-OPE-gly; (e)  $\text{CO}_2$  adsorption (195K) for both CMPs; (f) solid-state  $^{13}\text{C}$  NMR for TAPA-OPE-gly; (g) FE-SEM and (h) TEM images for TAPA-OPE-mix; (i) FE-SEM image for TAPA-OPE-gly; TEM images for TAPA-OPE-gly (j-m) - (j) nano-fibres in large area (k) lattice fringes; (l) high resolution TEM illustrating fibre opening site; (m) full length of a single nano-fibre.

morphology of the materials.<sup>[56, 57]</sup> This can be tuned and regulated by introducing long alky or glycol chain on the organic struts of the CMP materials.<sup>[58]</sup> However, there is no straight forward methodology for controlling nano-structuring in CMP materials. In this context, designing redox active CMPs by integration appropriate electron donor and acceptor organic moiety will lead to the facile charge migration and likely to show electro-catalytic activity.<sup>[6]</sup> At the same time, exploiting highly conjugated  $\pi$ -chromophoric spacer like *oligo*(*p*-phenyleneethynylenes) (OPEs) as the building block for CMP could exhibit excellent light harvesting property of the materials<sup>[46, 59, 60]</sup> which is prerequisite for the photocatalysis. Furthermore, presence of bola-amphiphilic (alkyl and alkoxy) side chain substitution on the struts will facilitate, in principle, in nano-structuring<sup>[29]</sup> and subsequently can accelerate the catalytic activity by providing exposed catalytic surfaces. Therefore, utilization of highly conjugated  $\pi$ -chromophoric struts with suitable side-chain substitutions for fabricating redox-active CMPs will be extremely relevant approach for the facile charge separation as well as migration which is fundamental requirement for both, electro and photo-catalysis.

In this article, we have designed and synthesized two redox-active CMPs (TAPA-OPE-mix and TAPA-OPE-gly) by integration of *N*1,*N*1-bis(4-aminophenyl)benzene-1,4-diamine (TAPA) and substituted

*oligo*(*p*-phenyleneethynylenes) (OPEs) (Scheme 1&S3) and have shown impressive heterogeneous catalytic activity for electro-chemical  $\text{O}_2$  reduction and photo-chemical  $\text{H}_2$  evolution reactions. Notably, TAPA is a well-studied electron donor and also known for the formation of long-lived charge-separated species.<sup>[61, 62]</sup> Whereas, OPEs is a large  $\pi$ -chromophoric multi-phenyl system that exhibit high light absorbing property and can act as electron acceptor. Moreover, asymmetric and symmetric side chain substitutions on bola amphiphilic OPE struts have resulted in irregular spherical and nano-tape morphologies of TAPA-OPE-mix and TAPA-OPE-gly, respectively. The TAPA-OPE-gly is found to be more hydrophilic due to the presence of di-glycol side chain in comparison to TAPA-OPE-mix as proven by solvent adsorption and consequently results in better electro- and photo-catalytic activity. Furthermore, *in-situ* stabilization of platinum nanoparticles on both CMPs resulted Pt@CMP nanocomposites which showed significantly high  $\text{H}_2$  evolution compared to the pristine CMPs.

## Results and Discussion

Both CMPs, TAPA-OPE-mix and TAPA-OPE-gly were synthesized in microwave condition by the Schiff base condensation

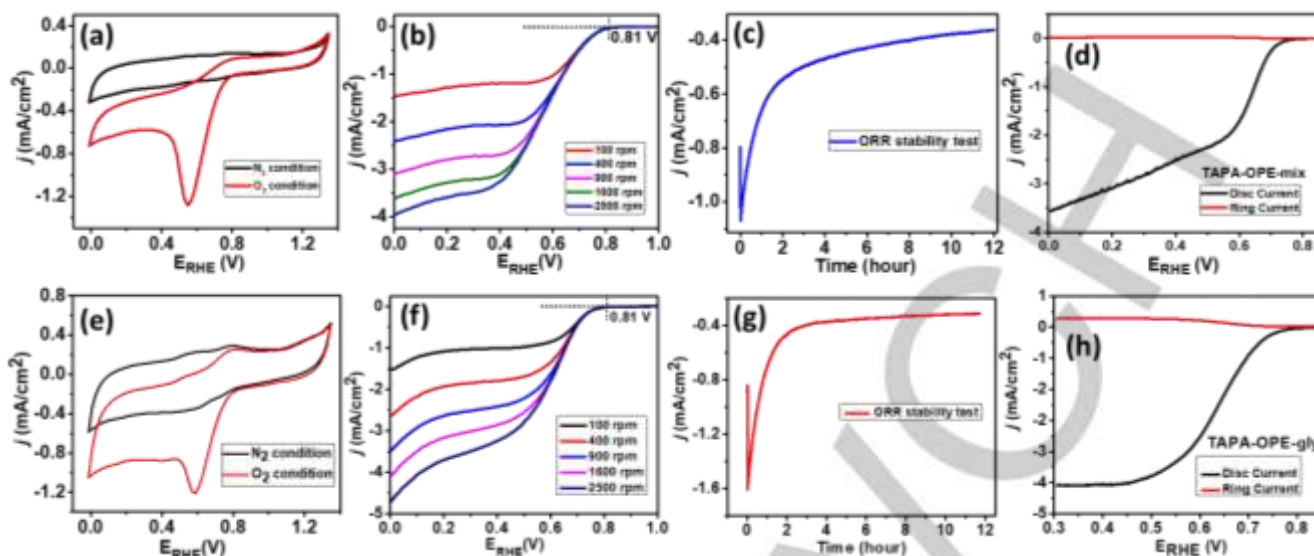


Figure 2: Electrocatalytic activity of both CMPs towards ORR: (a-d) for TAPA-OPE-mix – (a) CV; (b) LSV at different rpm; (c) catalytic stability for 12 hrs (d) RRDE plot. And (e-h) for TAPA-OPE-gly – (e) CV; (f) LSV at different rpm; (g) catalytic stability for 12 hrs (h) RRDE plot.

reaction between *N1,N1*-bis(4-aminophenyl)benzene-1,4-diamine (TAPA) and newly synthesized substituted *oligo*-(*p*-phenyleneethynylene)s (OPEs) namely; 4,4'-((2-(dodecyloxy)-5-(2-(2-(2-methoxyethoxy)ethoxy)ethoxy)-1,4-phenylene)bis(ethyne-2,1-diyl))dibenzaldehyde (for TAPA-OPE-mix) and 4,4'-((2,5-bis(2-(2-(2-methoxyethoxy)ethoxy)ethoxy)-1,4-phenylene)bis(ethyne-2,1-diyl))dibenzaldehyde (for TAPA-OPE-gly) (Scheme 1&S1-S3). Obtained CMPs were characterized by several spectroscopic and microscopic techniques (Figure 1). Porosity of CMPs was studied by gas adsorption experiment ( $N_2$  and  $CO_2$ ). The FT-IR spectrum for both CMPs are found to be similar due to similarities in the building units (Figure S3). An intense peak at  $1602$  and  $1605\text{ cm}^{-1}$  in TAPA-OPE-mix and TAPA-OPE-gly, respectively, are attributed to imine bond ( $-C=N$ ) and characteristics for the formation of polymers. A peak at  $2208\text{ cm}^{-1}$  correspond to alkyne bond ( $-C\equiv C-$ ) confirm the presence of OPE unit in both CMPs.<sup>[63]</sup> Solid state  $^{13}\text{C}$ -NMR spectra demonstrate a distinguish peak at  $154.2$  ppm for TAPA-OPE-mix and  $155.2$  ppm for TAPA-OPE-gly (Figure 1) which is attributed to the imine carbon ( $-C=N$ ) and confirm the formation of polymers. Notably, peaks between  $14$ – $29$  ppm and  $58.2$ – $70.4$  ppm in TAPA-OPE-mix are attributed to the alkyl and glycol carbons, respectively, confirming the presence of unsymmetrical side chain substitution in the polymer. Whereas, symmetrical substitution of glycol chain in OPE unit in the TAPA-OPE-gly exhibit peaks at  $58.3$  and  $70.9$  ppm. Powder-XRD performed for both CMPs in the range of  $3$  –  $35^\circ$  show a broad peak at  $2\theta = 21^\circ$  indicating the absence of long-range ordering in the polymers (Figure 1). Thermogravimetric analysis (TGA) indicated that both polymers are thermally stable up to  $300^\circ\text{C}$  without any significant weight loss (Figure S4). Afterwards, a gradual weight loss up to  $45\%$  was observed in both CMPs up to  $800^\circ\text{C}$ . Surface morphology of TAPA-OPE-mix studied by FE-SEM and showed an agglomerated irregular spherical morphology which has also been supported by TEM analysis (Figure 1). Whereas, FE-SEM analysis of TAPA-OPE-gly showed nano-tape like morphology

(Figure 1).<sup>[29]</sup> These nano-tapes were interconnected with each others and the length was found in the range of several micrometers. The width of nano-tapes was found to be  $70$  –  $80$  nm. This observation has been further validated by TEM studies (Figure 1). High resolution TEM (HR-TEM) analysis showed that the nano-tapes were folded at the edges and subsequently forming layered structures. Notably, an ordering was observed between layers with the spacing of  $3.69\text{ \AA}$  which typically indicates for the existence of  $\pi\cdots\pi$  interactions between them. The folding at edges are likely to be occurred due to repulsive interactions of hydrophilic symmetric side-chain substitutions (diglycol) on OPE bola-amphiphilic strut of TAPA-OPE-gly with hydrophobic solvents. However, different nano-structuring of TAPA-OPE-mix and TAPA-OPE-gly polymers can be attributed to the asymmetric and symmetric side-chain substitutions on OPE bola-amphiphilic struts, respectively.<sup>[29, 58]</sup> Here, tuning in morphology of materials is noteworthy and indeed a crucial factor for catalytic performances by the fact that nano-tapes structures provide more exposed catalytic surface area as compared to irregular spherical morphologies.<sup>[56, 57]</sup> More importantly, tuning of the morphology in CMP materials by subtle variation in substitutions is yet to be realized. UV-Vis absorption spectra of TAPA-OPE-mix and TAPA-OPE-gly in the solid state revealed that both CMPs exhibit broad absorbance in the range between  $250$  –  $600$  nm (Figure S8). Further, optical band gap calculated from UV-Vis absorption spectra was found to be  $2.38$  eV and  $2.35$  eV for TAPA-OPE-mix and TAPA-OPE-gly, respectively (Figure S9).

In order to investigate permanent porosity, gas adsorption studies ( $CO_2$  and  $N_2$ ) were performed for both CMPs (Figure 1&S5). Both CMPs were activated at  $150^\circ\text{C}$  for  $12$  h prior to sorption studies. Almost negligible  $N_2$  uptake ( $77$  K) in low pressure region followed by  $40$ – $50$  mL/g uptake at  $1$  atm pressure was observed for both CMPs (Figure S5). The high pressure  $N_2$  uptake could be attributed to the inter-particle void spaces. The presence of pendent alkyl or glycol chains on the pore surface of CMPs creates diffusion

barrier for  $N_2$  at 77K, thus decreased the low pressure uptake. Moreover,  $CO_2$  (195 K) uptake was found to be 60 – 65 mL/g up to 1 atm pressure for both CMPs (Figure 1). Type-I  $CO_2$  sorption profile for both CMPs is indicative for the micro-porous nature of polymers. However, polar  $CO_2$  molecules will diffuse easily through quadrupole interactions with several oxygen atoms present on the pore surfaces. Further, owing to the presence side chains of different polarity in CMPs, we have performed methanol sorption study (293 K) to understand the nature of interior pore surfaces. The methanol uptake in low pressure region (at 0.3 atm) for TAPA-OPE-mix and TAPA-OPE-gly was found to be 18 mL/g and 35 mL/g, respectively (Figure S6). This indicates for the facile diffusion of polar solvents in the TAPA-OPE-gly in comparison to TAPA-OPE-mix which could be attributed to the symmetric bola-amphiphilic substitutions (di-glycol) at the OPE unit in former CMP. Next, we were interested to investigate redox active behaviour of both CMPs in order to explore their catalytic applications (Figure S1&S2). Density functional theory (DFT) calculations were performed for repeating unit of both CMPs which showed that the electron density for highest occupied molecular orbital (HOMO) and lowest unoccupied molecular orbital (LUMO) were located at TAPA and OPE units, respectively. This indicates that the TAPA and OPE units act as electron donor and acceptor, respectively. The theoretical HOMO-LUMO band gap was found to be 2.34 and 2.36 eV for TAPA-OPE-mix and TAPA-OPE-gly, respectively, which is close agreement with the optical band-gap. Further, electron paramagnetic resonance (EPR) study was carried out for both CMPs in the solid state at room temperature. A sharp and intense signal at  $g = 1.949$  and  $1.942$  for TAPA-OPE-mix and TAPA-OPE-gly, respectively, is indicative formation of charge separated species at room temperature (Figure 1).<sup>[22]</sup> Thus, both theoretical and experimental studies unambiguously support for redox-active nature and subsequent formation of charge-separated species for both CMPs. Therefore, these CMPs can show interesting electro and photo-catalytic activity. Next, electrical conductivity was measured for both CMPs and showed semi-conducting nature with the conductivity value of  $8.1 \times 10^{-5} \text{ S cm}^{-1}$  and  $4.69 \times 10^{-5} \text{ S cm}^{-1}$  for TAPA-OPE-mix and TAPA-OPE-gly, respectively (Figure S7). Higher conductivity value for TAPA-OPE-gly in comparison to TAPA-OPE-mix could be attributed to the nano-tape morphology in former case.

The electro-catalytic activity for both CMPs were examined towards oxygen reduction reaction (ORR) (Figure 2). The ORR experiments were carried out in a three-electrode system in 0.1M KOH solution at the scan rate of 5 mV/s (see experimental section). Cyclic voltammetry (CV) in the  $O_2$  saturated solution showed an oxygen reduction peak at 0.54 V and 0.59 V with respect to reversible hydrogen electrode (RHE) for TAPA-OPE-mix and TAPA-OPE-gly, respectively (Figure 2). Notably, this peak was absent in  $N_2$  saturated solution which illustrates the electro-catalytic property of both CMPs towards reducing the  $O_2$ .<sup>[64]</sup> Further, we have performed linear sweep voltammetry (LSV) at different rotation speed at 5 mV/s scan rate for both CMPs (Figure 2). LSV curves for both CMPs illustrate similar onset potential of 0.81 V vs RHE. However, the current density at the maximum rotation speed of 2500 rpm is found to be 3.9 mA/cm<sup>2</sup> and 4.8 mA/cm<sup>2</sup> for TAPA-OPE-mix and TAPA-OPE-gly, respectively. Better catalytic activity of TAPA-OPE-gly as compared to TAPA-OPE-mix could be the combined effects of two factors; firstly nano-tape morphology provides exposed catalytic centre<sup>[57]</sup> and secondly more hydrophilic interior pores of TAPA-OPE-gly as confirmed by solvent adsorption is expected to facilitate

substrate transfer towards catalytic centre. Further, electrochemical impedance spectroscopic (EIS) study performed for CMPs (Figure S10). Electrode/electrolyte charge transfer resistance for TAPA-OPE-mix and TAPA-OPE-gly was found to be 150  $\Omega$  and 88  $\Omega$ , respectively, which further indicates for facile charge transfer in the TAPA-OPE-gly.<sup>[65]</sup> Number of electrons transferred to the per oxygen centre during the ORR was calculated by the Koutechy–Levich (K-L) equation (Figure S11). A good linearity in the range of 0.3 to 0.5 V demonstrate first order kinetics for both CMPs and number of electron (n) transferred to per oxygen centre were found to be 3.68 – 3.79, indicating for four-electron transfer during the ORR process. The RRDE experiment was performed to understand the formation

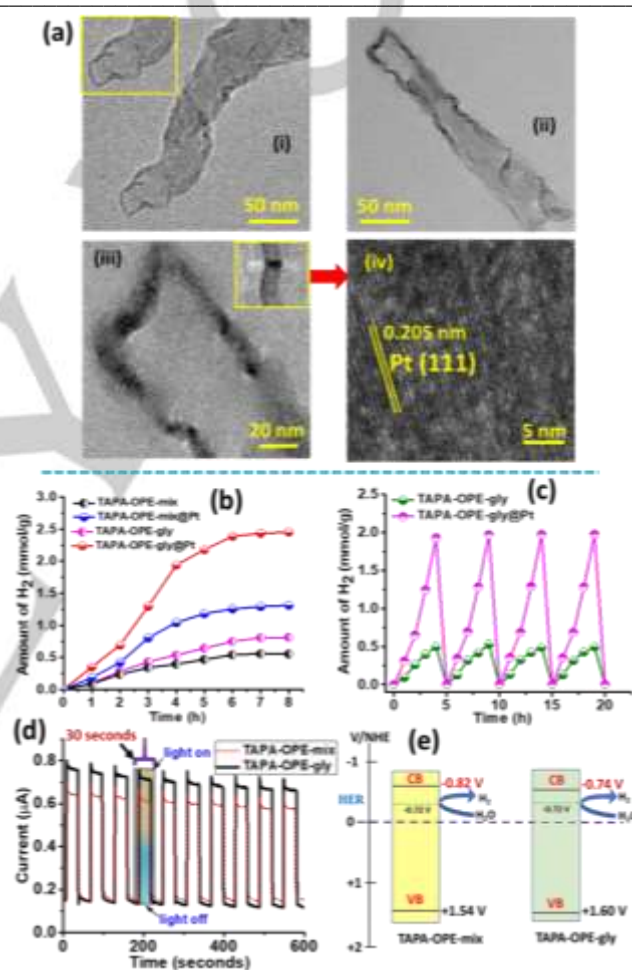


Figure 3: Photocatalytic  $H_2$  evolution for both CMPs: (a) TEM images before and after Pt nano-particles stabilization in TAPA-OPE-gly – (i) HR-TEM for TAPA-OPE-gly; (ii) HR-TEM for Pt@TAPA-OPE-gly, inset shows presence of Pt nanoparticles; (iii) TEM image for Pt@TAPA-OPE-gly in large area; (iv) lattice fringes for Pt nanoparticles; (b) Photocatalytic  $H_2$  evolution performances for both CMPs as well as Pt@CMPs upon light irradiation (full-range); (c) recyclability test for photocatalyst TAPA-OPE-gly and Pt@TAPA-OPE-gly for four cycles; (d) photocurrent generation upon light “ON” and “OFF” for TAPA-OPE-mix and TAPA-OPE-gly for 10 cycles; (e) schematic presentation of Mott-Schottky plot for illustrating thermodynamic feasibility of CMPs towards photocatalytic  $H_2$  evolution.

of  $\text{H}_2\text{O}_2$  as the by-product of partial  $\text{O}_2$  reduction during the ORR. The amount of  $\text{H}_2\text{O}_2$  generated during ORR at the potential of 0.25 V wrt RHE was found to be around 12 and 15% for TAPA-OPE-mix and TAPA-OPE-gly, respectively. Further, the number of electrons transferred to oxygen is calculated by RRDE and found to be 3.78 – 3.93 (Figure S12) which further supports for the four-electron transfer. The chrono-amperometry experiment was performed for both CMPs at the static potential of 0.3 V for 12 h to evaluate the catalytic stability. After initial current stabilization within an hour, the current density was found to be retained more than 90% for both CMPs which showed excellent catalytic stability (Figure 2). We have theoretically predicted oxygen binding site with TAPA-OPE-gly during ORR (Figure S13). We observed that  $\text{O}_2$  binding at the central nitrogen of TAPA centre is stabilized by -2.59 Kcal/mol and therefore TAPA could serve as the catalytic centre for ORR. Furthermore, a plausible mechanism for ORR has been elucidated theoretically<sup>[66, 67]</sup> and given in the supporting information in detail (scheme S4).

Photocatalytic studies for both CMPs were performed towards water splitting using 300 W xenon lamp in both, full range (280 – 750 nm) as well as visible light (400 – 750 nm) irradiation (see SI for detail). The screening of sacrificial reagents using TAPA-OPE-mix indicated that the mixture of 0.1 M sodium sulphate and 0.2 M sodium sulphide served the best hole scavenger among all others and yielded highest amount of  $\text{H}_2$  gas under similar condition (228  $\mu\text{mol/g}$  in 2 hours in full range) (Figure 14). Therefore, this mixture has been utilized further as a sacrificial agent for all the photocatalytic  $\text{H}_2$  evolution studies. The amount of  $\text{H}_2$  evolved during photocatalysis was quantified in regular time-interval using gas chromatography. The  $\text{H}_2$  production upon irradiation with full range of light (280-750 nm) was reached to saturation in 8 h for both CMPs and subsequent  $\text{H}_2$  evolution was found to be 540  $\mu\text{mol}$  and 820  $\mu\text{mol}$  for TAPA-OPE-mix and TAPA-OPE-gly, respectively (Figure 3). Further, recyclability of catalyst was investigated for four cycles in the time interval of four hours. After every 4 h, reaction mixture was purged with  $\text{N}_2$  gas for almost 30 minutes followed by GC-MS analysis to ensure complete removal of  $\text{H}_2$  gas. The consistent  $\text{H}_2$  evolution for four cycles is indicative for stable catalytic performances for both CMPs (Figure 2&S15). Further, photocatalytic activity investigated for both CMPs upon visible light (400 – 750 nm) irradiation for 6 hrs and  $\text{H}_2$  evolution was observed in the range of 40 – 55  $\mu\text{mol}$  (Figure S16). Next, photocurrent study was performed with both CMPs upon consecutive light ON-OFF for 30 seconds for 10 cycles (Figure 3). The photo-current for TAPA-OPE-mix and TAPA-OPE-gly was found to be 0.65  $\mu\text{A}$  and 0.76  $\mu\text{A}$  upon light "ON" and 0.16  $\mu\text{A}$  and 0.15  $\mu\text{A}$  upon light "OFF", respectively. The photocurrent study revealed unambiguously that the charge transfer process is significantly higher in the TAPA-OPE-gly as compared to TAPA-OPE-mix. This is noteworthy by the fact that the 1D nano-tape morphology of TAPA-OPE-gly is expected to facilitate the higher charge mobilization in comparison to the irregular spherical morphology of TAPA-OPE-mix. Further, the average rate of hydrogen evolution was calculated to be  $\sim 88.3 \mu\text{mol/h/g}_{\text{cat}}$  for TAPA-OPE-mix and  $\sim 124.3 \mu\text{mol/h/g}_{\text{cat}}$  for TAPA-OPE-gly. Next, the turn over number (TON) calculated for TAPA-OPE-mix and TAPA-OPE-gly was found to be 0.71 and 1.02, respectively. The TON values are unambiguously indicative for better photocatalytic activity for TAPA-OPE-gly compared to TAPA-OPE-mix which is well supported through morphology, impedance and photo-current studies.

Further, mechanistic insight of photocatalytic activity for both, TAPA-OPE-mix and TAPA-OPE-gly was investigated by Mott-Schottky plot analysis (Figure S17). Mott-Schottky plot has demonstrated the n-type semiconducting nature for both CMPs. Notably, the conduction band edge potential for TAPA-OPE-mix and TAPA-OPE-gly calculated from Mott-Schottky plot was found to be -0.82 V and -0.74 V which is more negative than the required potential for water splitting (-0.72 V) at pH = 12.2 (Figure S17). This provides an experimental validation for photocatalytic activity of both CMPs.

We have previously reported that in-situ stabilization of metal nanoparticles like Co in a TAPA containing porous matrix for enhanced electrocatalytic activity.<sup>[22]</sup> Further, with the aim to increase the  $\text{H}_2$  evolution, we envisioned that the in-situ stabilization of Pt nanoparticles on the CMP matrices could be advantageous as the photogenerated electron can be easily reach to the surface attached Pt nanoparticles without recombination.<sup>[68]</sup> Thus, we have in-situ stabilized Pt nanoparticles in the CMP matrices (see experimental section) which was confirmed by TEM analysis, EDAX and elemental mapping (Figure 3, S18-S20). The quantification of Pt nano-particles in CMP matrix was done by elemental mapping, EDAX, and ICP analysis that support for presence of  $\sim 6 \text{ wt\%}$  and  $\sim 8 \text{ wt\%}$  Pt nanoparticles in the TAPA-OPE-mix and TAPA-OPE-gly, respectively (Figure S20). FE-SEM and TEM analysis revealed that Pt nano-particles were embedded in the polymer matrix (Pt@TAPA-OPE-mix and Pt@TAPA-OPE-gly) with maintaining the original morphology of bare CMPs. Interestingly, HR-TEM analysis showed ordering in Pt nano-particles and corresponding lattice fringes was found to be 2.13 Å and 2.05 Å for Pt@TAPA-OPE-mix and Pt@TAPA-OPE-gly, respectively, which indicates for the presence of Pt (111) in both CMPs (Figure 3&S19). Next, photocatalytic performances were examined for both Pt@CMPs. The amount of  $\text{H}_2$  obtained after Pt nanoparticle stabilization was found to be significantly higher in comparison to bare CMPs (Figure 3). The amount of  $\text{H}_2$  obtained from Pt@TAPA-OPE-mix and Pt@TAPA-OPE-gly was found to be 1200  $\mu\text{mol}$  and 2500  $\mu\text{mol}$  in 8 hours in the full-range which is almost three times higher as compared to bare CMPs. The average rate of hydrogen evolution for Pt@TAPA-OPE-mix and Pt@TAPA-OPE-gly was found to be  $\sim 209.7 \mu\text{mol/h/g}_{\text{cat}}$  and  $\sim 399.2 \mu\text{mol/h/g}_{\text{cat}}$ , respectively. The better photo-catalytic performance of Pt@TAPA-OPE-gly could be attributed to the ordered nano-tape morphology that is expected to provide more exposed catalytic surfaces in comparison to the Pt@TAPA-OPE-mix. The recyclability of Pt@TAPA-OPE-mix and Pt@TAPA-OPE-gly was investigated similar to bare CMPs. Consistent performance of platinum stabilized polymers for four cycles indicated for the impressive catalytic recyclability for both Pt@CMP nanocomposites (Figure 3).

## Conclusions

In this work, we have synthesized two new redox-active CMPs; TAPA-OPE-mix and TAPA-OPE-gly using microwave technique and explored their bimodal catalytic activities towards electrochemical ORR and photochemical HER processes. Interestingly, the catalytic activities of CMPs were enhanced by

regulating nano-structuring through modulating side-chain substitutions of the organic struts. Notably, asymmetric (alkyl/glycol) and symmetric (di-glycol) side-chain substitutions on OPE bola amphiphilic struts of TAPA-OPE-mix and TAPA-OPE-gly, respectively, have resulted in more polar interior surface for later one as confirmed by methanol adsorption. Further, as the result of different side-chain substitutions of OPE, these CMPs exhibit distinct nano-structures which play a crucial role in materials properties. Both CMPs have shown potential for electrocatalytic oxygen reduction with an onset potential of 0.81 V. The maximum current density at the rotation speed of 2500 rpm was found to be 3.9 mA/cm<sup>2</sup> and 4.8 mA/cm<sup>2</sup> for TAPA-OPE-mix and TAPA-OPE-gly, respectively. Furthermore, TAPA-OPE-mix and TAPA-OPE-gly have shown impressive photocatalytic activity towards H<sub>2</sub> evolution with the value of 540 μmol and 820 μmol, respectively. Moreover, *in-situ* platinum (Pt) nano-particles stabilization in CMPs accelerate the H<sub>2</sub> evolution for more than three times. Photocurrent studies showed that the charge transfer is faster for TAPA-OPE-gly as compared to TAPA-OPE-mix. Further, Mott-schotky plot analysis validated the photocatalytic activity for both CMPs towards H<sub>2</sub> evolution. Thus, present work paves a new way to realize bimodal heterogeneous catalytic properties in a porous organic polymer materials.

## Experimental Section:

**Synthesis:** Synthetic procedure used for the synthesis of OPE based dialdehydes (ALD1 and ALD2) was similar to the literature reported (detail is given in the supporting information (SI), Figure S1-S3). However, both CMPs were synthesized using microwave synthesizer and detail procedure is given below;

**(a) Synthesis of CMPs (TAPA-OPE-mix and TAPA-OPE-gly):** Both CMPs have been synthesized by Schiff based condensation reaction using reported procedure. Interestingly, we have performed CMPs synthesis using micro-wave reactor which required significantly lesser time and gives impressive yield in comparison to solvothermal method. The OPE based di-aldehyde; 4,4'-((2-(dodecyloxy)-5-(2-(2-methoxyethoxy)ethoxy)ethoxy)-1,4-phenylene)bis(ethyne-2,1-diyl)dibenzaldehyde (ALD1) and 4,4'-((2,5-bis(2-(2-(2-methoxyethoxy)ethoxy)ethoxy)-1,4-phenylene)bis(ethyne-2,1-diyl)dibenzaldehyde (ALD2) was used for the synthesis of TAPA-OPE-mix and TAPA-OPE-gly, respectively. In brief, OPE based dialdehyde (0.197 mmol) and 4,4',4''-triaminotriphenylamine (TAPA) (0.132 mmol) were taken together in the mixture of mesitylene (0.75 mL) and 1,4-dioxane solvent (0.5 mL). Then catalytic amount of 6M acetic acid (150 μl) was added into it. The reaction mixture was heated in the microwave reactor at 120°C for 2 hours. The reaction mixture was cooled to room temperature and subsequently washed with 1,4-dioxane and methanol three times. The obtained CMP materials were purified by Soxhlation performed in THF for two days. Both CMPs were found to be orange-red in colour. Purified CMPs was dried at 120 °C for 12 h. The yield of pure TAPA-OPE-mix and TAPA-OPE-gly was found to be 75 – 80 %.

**(b) In-situ generation and stabilization of Pt nanoparticles in CMP matrix:** We have used similar procedure as reported earlier for in-situ stabilization of Pt nanoparticles.<sup>[69]</sup> In brief, 1 mg of H<sub>2</sub>PtCl<sub>6</sub>·6H<sub>2</sub>O was taken in 40 ml of water followed by addition of 5 mg of CMP. After continuous stirring for 1 h in a closed system, the well-dispersed solution was irradiated for 2 h using 300 W xenon

lamp (Newport) with a 6.0 cm long IR water filter. Finally, the Pt stabilized CMP materials (Pt@CMP) was obtained which have been washed thoroughly with deionized (DI) water and dried in air.

**Electrocatalysis:** Instrumental set-up and experimental condition is described in detail in the supporting information. In brief, the glassy carbon, Hg/HgO and platinum electrodes were used as working, reference and counter electrodes, respectively. All the electrochemical experiments were performed using 0.1 M KOH solution as electrolyte. The electrocatalytic ink was prepared by mixing CMP material (2.5 mg) and volcan carbon (2.5 mg) in 1 mL solvent which is mixture of isopropyl alcohol (493 μL), milliQ water (493 μL) and Nafion (14 μL). A good dispersion of electrocatalytic ink was prepared by sonicating the mixture for 45 minutes. Next, freshly prepared ink (3.5 μL) was drop costed over working electrode and left for around 3 hours under ambient condition for drying. All the ORR experiments were studied in rotating disc electrode (RDE) voltammetry. However, rotating ring disc electrode (RRDE) voltammetry experiment was performed in order to confirm and quantify the H<sub>2</sub>O<sub>2</sub> evolution during ORR. Linear sweep voltammetry (LSV) experiments was performed in RDE at different rotation speed; 100, 400, 900, 1600, 2500 rpm with the constant scan rate of 5 mV/s. Notably, electrocatalytic activity of bare volcan carbon was also examined toward ORR. The electrocatalytic activity of volcan carbon was found to be negligible (current density was less than 1 mA/cm<sup>2</sup>) in comparison to CMPs. This showed that the electrocatalytic activity of the prepared ink is attributed to the CMP materials.

**Photocatalysis:** The similar procedure for sample preparation was employed during photocatalytic studies for bare as well as Pt stabilized CMPs. For the photocatalysis, 2 mg of CMP material was dispersed in 10 mL acetonitrile. Separately, a mixture of sodium sulphate (0.1 M) and sodium sulphide (0.2 M) was prepared in 30 mL water and added to the dispersed solution of CMP. The reaction mixture was purged with N<sub>2</sub> gas approximately for 30 minutes followed by GC-analysis to ensure the absence of H<sub>2</sub> gas in the solution. This reaction mixture is used for photocatalysis.

## Acknowledgements

AS thanks SERB, DST, India for National Post-Doctoral Fellowship (SERB project No. PDF/2016/002324). TKM is grateful to the DST (Project No. TRC-DST/C.14.10/16-2724), Govt. of India and JNCASR for financial support.

**Keywords:** conjugated microporous polymer, bimodal electro and photo-catalyst, oxygen reduction, hydrogen evolution, platinum nanoparticles.

## References

- [1] Z. W. Seh, J. Kibsgaard, C. F. Dickens, I. Chorkendorff, J. K. Nørskov, T. F. Jaramillo, *Science* **2017**, *355*, eaad4998.
- [2] M. Rana, S. Mondal, L. Sahoo, K. Chatterjee, P. E. Karthik, U. K. Gautam, *ACS Appl. Mater. Interfaces* **2018**, *10*, 33737 – 33767.
- [3] M. K. Debe, *Nature* **2012**, *486*, 43 - 51.
- [4] J. Yang, X. Wang, B. Li, L. Ma, L. Shi, Y. Xiong, H. Xu, *Adv. Funct. Mater.* **2017**, *27*, 1606497 - 1606507.

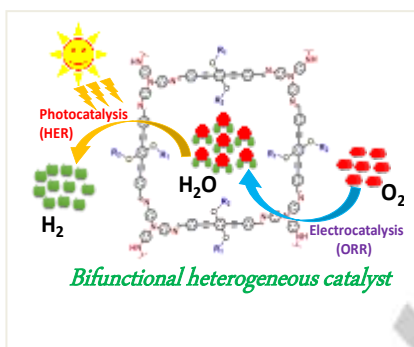
- [5] W.-J. Yin, B. Weng, J. Ge, Q. Sun, Z. Li, Y. Yan, *Energy Environ. Sci.* **2019**, *12*, 442 - 462.
- [6] S. Roy, A. Bandyopadhyay, M. Das, P. P. Ray, S. K. Pati, T. K. Maji, *J. Mater. Chem. A* **2018**, *6*, 5587 - 5591.
- [7] S. Yang, Y. Yu, M. Dou, Z. Zhang, L. Dai, F. Wang, *Angew. Chem. Int. Ed.* **2019**, *58*, 14724 - 14730.
- [8] Y. Li, H. Dai, *Chem. Soc. Rev.* **2014**, *43*, 5257 - 5275.
- [9] T. Jafari, E. Moharrerri, A. S. Amin, R. Miao, W. Song, S. L. Suib, *Molecules* **2016**, *21*, 900 - 928.
- [10] K. Maeda, K. Domen, *J. Phys. Chem. Lett.* **2010**, *1*, 2655 - 2661.
- [11] Z. Wang, C. Li, K. Domen, *Chem. Soc. Rev.* **2019**, *48*, 2109 - 2125.
- [12] C. Acar, I. Dincer, G. F. Naterer, *Int. J. Energy Res.* **2016**, *40*, 1449 - 1473.
- [13] J. Huo, Y.-B. Zhang, W.-Y. Zou, X. Hu, Q. Deng, D. Chen, *Catal. Sci. Technol.* **2019**, *9*, 2716 - 2727.
- [14] Q. Lu, Y. Yu, Q. Ma, B. Chen, H. Zhang, *Adv. Mater.* **2016**, *28*, 1917 - 1933.
- [15] D. Z. Zee, T. Chantarojsiri, J. R. Long, C. J. Chang, *Acc. Chem. Res.* **2015**, *48*, 2027 - 2036.
- [16] L. Zhang, K. Doyle-Davis, X. Sun, *Energy Environ. Sci.* **2019**, *12*, 492 - 517.
- [17] J. Yang, D. Wang, H. Han, C. Li, *Acc. Chem. Res.* **2013**, *46*, 1900 - 1909.
- [18] S. Elmas, W. Beelders, S. J. Bradley, R. Kroon, G. Laufersky, M. Andersson, T. Nann, *ACS Sustainable Chem. Eng.* **2017**, *5*, 10206 - 10214.
- [19] A. Ganguly, O. Anjaneyulu, K. Ojha, A. K. Ganguli, *CrystEngComm* **2015**, *17*, 8978 - 9001.
- [20] B. Y. Xia, Y. Yan, N. Li, H. B. Wu, X. D. Lou, X. Wang, *Nat. Energy* **2016**, *1*, 15006.
- [21] N. Sikdar, B. Konkena, J. Masa, W. Schuhmann, T. K. Maji, *Chem. Eur. J.* **2017**, *23*, 1-9.
- [22] A. Singh, D. Samanta, T. K. Maji, *ChemElectroChem* **2019**, *6*, 3756 - 3763.
- [23] J. Liang, Y. Jiao, M. Jaroniec, S. Z. Qiao, *Angew. Chem. Int. Ed.* **2012**, *51*, 11496 - 11500.
- [24] S. Bhattacharyya, C. Das, T. K. Maji, *RSC Adv.* **2018**, *8*, 26728 - 26754.
- [25] H. X. Zhong, J. Wang, Y. W. Zhang, W. L. Xu, W. Xing, D. Xu, Y. F. Zhang, X. B. Zhang, *Angew. Chem. Int. Ed.* **2014**, *53*, 14235-14239.
- [26] H. Jin, C. Guo, X. Liu, J. Liu, A. Vasileff, Y. Jiao, Y. Zheng, S.-Z. Qiao, *Chem. Rev.* **2018**, *118*, 6337 - 6408.
- [27] S. Bai, Y. Xiong, *Chem. Commun.* **2015**, *51*, 10261 - 10271.
- [28] L. Dai, Y. Xue, L. Qu, H.-J. Choi, J.-B. Baek, *Chem. Rev.* **2015**, *115*, 4823 - 4892.
- [29] D. Samanta, P. Verma, S. Roy, T. K. Maji, *ACS Appl. Mater. Interfaces* **2018**, *10*, 23140 - 23146.
- [30] J.-L. Wang, C. Wang, W. Lin, *ACS Catal.* **2012**, *2*, 2630 - 2640.
- [31] L. Chen, Y. Honsho, S. Seki, D. Jiang, *J. Am. Chem. Soc.* **2010**, *132*, 6742 - 6748.
- [32] Y. Bai, L. Wilbraham, B. J. Slater, M. A. Zwiijnenburg, R. S. Sprick, A. I. Cooper, *J. Am. Chem. Soc.* **2019**, *141*, 9063 - 9071.
- [33] H. Zhu, D. Liu, D. Zou, J. Zhang, *J. Mater. Chem. A* **2018**, *6*, 6130 - 6154.
- [34] Y. Xu, M. Kraft, R. Xu, *Chem. Soc. Rev.* **2016**, *45*, 3039 - 3052.
- [35] S. Das, P. Heasman, T. Ben, S. Qiu, *Chem. Rev.* **2017**, *117*, 1515 - 1563.
- [36] P. Kaur, J. T. Hupp, S. T. Nguyen, *ACS Catal.* **2011**, *1*, 819 - 835.
- [37] S. M. J. Rogge, A. Bavykina, J. Hajek, H. Garcia, A. I. Olivoso-Suarez, A. S. Iveda-Escribano, A. Vimont, G. Clet, P. Bazin, F. Kapteijn, M. Daturi, E. V. Ramos-Fernandez, F. X. L. i. Xamena, V. V. Speybroeck, J. Gascon, *Chem. Soc. Rev.* **2017**, *46*, 3134 - 3184.
- [38] P. Pachfule, A. Acharjya, J. m. Roeser, T. Langenhahn, M. Schwarze, R. Schomacker, A. Thomas, J. Schmidt, *J. Am. Chem. Soc.* **2018**, *140*, 1423 - 1427.
- [39] Y. Xu, S. Jin, H. Xu, A. Nagai, D. Jiang, *Chem. Soc. Rev.* **2013**, *42*, 8012 - 8031.
- [40] A. I. Cooper, *Adv. Mater.* **2009**, *21*, 1291 - 1295.
- [41] S. Bhattacharyya, D. Samanta, S. Roy, V. P. H. Radhakantha, T. K. Maji, *ACS Appl. Mater. Interfaces* **2019**, *11*, 5455 - 5461.
- [42] S. A. Bhat, C. Das, T. K. Maji, *J. Mater. Chem. A* **2018**, 19834 - 19842.
- [43] A. Singh, D. Samanta, M. Boro, T. K. Maji, *Chem. Commun.* **2019**, 2837 - 2840.
- [44] C. Gu, N. Huang, Y. Chen, L. Qin, H. Xu, S. Zhang, F. Li, Y. Ma, D. Jiang, *Angew. Chem. Int. Ed.* **2015**, *54*, 13594 - 13598.
- [45] J.-X. Jiang, A. Trewin, D. J. Adams, A. I. Cooper, *Chem. Sci.* **2011**, *2*, 1777 - 1781.
- [46] S. Roy, D. Samanta, S. Bhattacharyya, P. Kumar, A. Hazra, T. K. Maji, *J. Phys. Chem. C* **2018**, *122*, 21598 - 21606.
- [47] V. M. Suresh, S. Bonakala, S. Roy, S. Balasubramanian, T. K. Maji, *J. Phys. Chem. C* **2014**, *118*, 24369 - 24376.
- [48] R. S. Sprick, J.-X. Jiang, B. Bonillo, S. Ren, T. Ratvijitvech, P. Guiglion, M. A. Zwiijnenburg, D. J. Adams, A. I. Cooper, *J. Am. Chem. Soc.* **2015**, *137*, 3265 - 3270.
- [49] V. S. Mothika, P. Sutar, P. Verma, S. Das, S. K. Pati, T. K. Maji, *Chem. Eur. J.* **2019**, *25*, 3867 - 3874.
- [50] G. Mukherjee, J. Thote, H. B. Aiyappa, S. Kandambeth, S. Banerjee, K. V. and, R. Banerjee, *Chem. Commun.* **2017**, 53, 4461 - 4464.
- [51] R. S. Sprick, B. Bonillo, M. Sachs, R. Clowes, J. R. Durrant, D. J. Adams, A. I. Cooper, *Chem. Commun.* **2016**, 52, 10008 - 10011.
- [52] N. M. Padial, J. Castells-Gil, N. Almora-Barrios, M. Romero-Angel, I. d. Silva, M. Barawi, A. Garcia-Sanchez, V. A. d. I. P. a. O'Shea, C. Marti-Gastaldo, *J. Am. Chem. Soc.* **2019**, *141*, 13124 - 13133.
- [53] S. Wei, F. Zhang, W. Zhang, P. Qiang, K. Yu, X. Fu, D. Wu, S. Bi, F. Zhang, *J. Am. Chem. Soc.* **2019**, *141*, 14272 - 14279.
- [54] B. P. Biswal, H. A. Vignolo-Gonzalez, T. Banerjee, L. Grunenberg, G. k. Savasci, K. Gottschling, J. r. Nuss, C. Ochsenfeld, B. V. Lotsch, *J. Am. Chem. Soc.* **2019**, *141*, 11082 - 11092.
- [55] W. Wang, X. Xu, W. Zhou, Z. Shao, *Adv. Sci.* **2017**, *4*, 1600371 - 1600391.
- [56] C. Zhou, X. Feng, R. Wang, G. Yang, T. Wang, J. Jiang, *ACS Omega* **2018**, *3*, 10638 - 10646.
- [57] L. Yang, M. Wang, P. M. Slattum, B. R. Bunes, Y. Wang, C. Wang, L. Zang, *ACS Appl. Mater. Interfaces* **2018**, *10*, 19764 - 19772.
- [58] K. Balakrishnan, A. Datar, T. Naddo, J. Huang, R. Oitker, M. Yen, J. Zhao, L. Zang, *J. Am. Chem. Soc.* **2006**, *128*, 7390 - 7398.
- [59] D. Samanta, A. Singh, P. Verma, S. Bhattacharyya, S. Roy, T. K. Maji, *J. Org. Chem.* **2019**, *84*, 10946 - 10952.
- [60] S. Roy, D. Samanta, P. Kumar, T. K. Maji, *Chem. Commun.* **2018**, *54*, 275 - 278.
- [61] P. Blanchard, C. Malacrid, C. Cabanetos, J. Roncali, S. Ludwigs, *Polym Int* **2019**, *68*, 589 - 606.

- [62] S.-H. Hsiao, W.-K. Liao, G.-S. Liou, *Polym. Chem.* **2018**, *9*, 236 - 248.
- [63] A. Singh, S. Roy, C. Das, D. Samanta, T. K. Maji, *Chem. Commun.*, **2018**, *54*, 4465 - 4468.
- [64] S. Bhattacharyya, B. Konkena, K. Jayaramulu, W. Schuhmann, T. K. Maji, *J. Mater. Chem. A* **2017**, *5*, 13573 - 13580.
- [65] Y. Liu, W. Wang, Y. Ying, Y. Wang, X. Peng, *Dalton Trans.* **2015**, *44*, 7123 - 7126.
- [66] H. B. Tao, J. Zhang, J. Chen, L. Zhang, Y. Xu, J. G. Chen, B. Liu, *J. Am. Chem. Soc.* **2019**, *141*, 13803 - 13811.
- [67] R. Ma, G. Lin, Y. Zhou, Q. Liu, T. Zhang, G. Shan, M. Yang, J. Wang, *NPJ Comput. Mater.* **2019**, *5*, 1 - 15.
- [68] A. J. Olaya, T. Omatsu, J. C. Hidalgo-Acosta, J. S. Riva, V. C. Bassetto, N. Gasilova, H. H. Girault, *J. Am. Chem. Soc.* **2019**, *141*, 6765 - 6774.
- [69] A. Razzaq, A. Sinhamahapatra, T.-H. Kang, C. A. Grimes, J.-S. Yu, S.-I. In, *Appl. Catal., B.* **2017**, *215*, 28 - 35.

## Table of Contents

## FULL PAPER

**Bifunctional (Electro/Photo) catalyst:** Bimodal functionality towards electrochemical  $O_2$  reduction and photochemical  $H_2$  evolution of donor-acceptor based redox-active conjugated microporous polymers (CMPs) has been explored. Notably, tuning the side-chain substitutions on OPE bola-amphiphilic struts showed distinct nano-structuring in CMPs that has high impact on catalytic performances.



Ashish Singh, Parul Verma, Debabrata Samanta, Tarandeep Singh and Tapas Kumar Maji\*

Page No. – Page No.

**Bimodal heterogeneous functionality in redox-active conjugated microporous polymer towards electrocatalytic oxygen reduction and photocatalytic hydrogen evolution**